Fundamental Research 3 (2023) 322–331

Contents lists available at ScienceDirect

Fundamental Research

journal homepage: http://www.keaipublishing.com/en/journals/fundamental-research/

Review

Recent progress in the theoretical design of two-dimensional ferroelectric materials

Xin Jin[a], Yu-Yang Zhang[a], Shixuan Du[a,b,*]

[a] University of the Chinese Academy of Sciences and Institute of Physics, Chinese Academy of Sciences, Beijing 100190, China
[b] Songshan Lake Materials Laboratory, Dongguan, Guangdong 523808, China

ARTICLE INFO

Article history:
Received 30 August 2022
Received in revised form 11 January 2023
Accepted 2 February 2023
Available online 2 March 2023

Keywords:
Ferroelectric
Ferroelectric functional devices
Two-dimensional
Theoretical design
First-principles

ABSTRACT

Two-dimensional (2D) ferroelectrics (FEs), which maintain stable electric polarization in ultrathin films, are a promising class of materials for the development of various miniature functional devices. In recent years, several 2D FEs with unique properties have been successfully fabricated through experiments. They have been found to exhibit some unique properties either by themselves or when they are coupled with other functional materials (e.g., ferromagnetic materials, materials with 5*d* electrons, etc.). As a result, several new types of 2D FE functional devices have been developed, exhibiting excellent performance. As a type of newly discovered 2D functional material, the number of 2D FEs and the exploration of their properties are still limited and this calls for further theoretical predictions. This review summarizes recent progress in the theoretical predictions of 2D FE materials and provides strategies for the rational design of 2D FE materials. The aim of this review is to provide guidelines for the design of 2D FE materials and related functional devices.

1. Introduction

Ferroelectrics (FEs), a type of functional material characterized by spontaneous electric polarization that can be reversed by an external electric field, have been the subject of extensive research in both fundamental science and device applications since their discovery in 1920 by Valasek [1]. From a fundamental science perspective, the phase transition, domain dynamics, and coupling among ferroic orderings (ferroelectric, ferromagnetic, ferroelastic) are of significant interest. In terms of device applications, FEs have gained considerable attention due to their potential for use in electronic devices. For example, by sandwiching a FE layer between two electrodes, a kind of nonvolatile memory named ferroelectric tunnel junction (FTJ) forms, where the two FE polarization states represent the two logic states ("0″ and "1″) and are electrically manipulable and readable [2,3]. Ferroelectric field-effect transistors (FeFETs), which integrate FEs into traditional FETs as a dielectric layer, enable in-memory computing [4]. Additionally, due to their piezoelectric and optoelectronic properties, FEs also show potential in electromechanical and photovoltaic devices [5,6]. The unique properties and various applications of ferroelectrics make it a crucial field of study in modern material science.

The miniaturization of electronic devices as a result of advancements in the microelectronics industry has presented new challenges for ferroelectrics (FEs), particularly in regards to size reduction of materials. The most commonly used type of FE, perovskite FEs, often suffer from polarization instability when the thickness is reduced to a few nanometers due to enhanced depolarization field, surface reconstructions, and defects [7–9]. Significant progress has been made in solving these problems, and several achievements have been made. For example, stable ultrathin ferroelectric $PbTiO_3$ (3 unit cell thick) [10], $BaTiO_3$ (4 unit cell thick) [11], $BiFeO_3$ (1–3 unit cell thickness) [12,13] have been successfully fabricated in experiments. However, it should be noted that complex fabrication processes are required to obtain high-quality ferroelectric perovskite thin films, and their properties are highly sensitive to interface lattice mismatch; thus, specific kinds of substrate are required. Such difficulties have motivated researchers to search for and design new types of ultrathin FE materials.

The successful exfoliation of graphene from graphite by Novoselov et al. in 2004 marked the beginning of a new research field in two-dimensional (2D) materials [14–19]. 2D materials are typically defined as crystalline materials with thicknesses down to single- or few-layer, where in-plane atoms are bonded by strong covalent bonds, and adjacent layers are bonded by weak van der Waals (vdW) interactions. The emergence of 2D materials provides new opportunities for the development of ultrathin FE materials. However, in the first decade of research in 2D materials, studies on 2D FE materials were absent, as most of

* Corresponding author.
E-mail address: sxdu@iphy.ac.cn (S. Du).

https://doi.org/10.1016/j.fmre.2023.02.009

the discovered 2D materials, such as graphene, h-BN, transition metal dichalcogenides (TMDs), and MXene, have centrosymmetric structures along the z-direction, prohibiting the emergence of out-of-polarization. The in-plane polarization is also prohibited owing to the rotation symmetry. However, in 2016, two types of 2D materials, SnTe [20] and $CuInP_2S_6$ [21], were experimentally verified to preserve stable in-plane and out-of-plane polarization when their thicknesses were reduced to a few nanometers, marking the discovery of 2D FE materials. To date, more than ten kinds of 2D FE materials have been successfully fabricated and several 2D FE-based electronic devices with excellent performance have also been realized.

Despite their ultrathin thickness and stable polarization, 2D FE materials also possess unique properties compared to traditional bulk perovskite ferroelectrics. The weak interlayer interactions in 2D FEs result in clean surfaces with minimal dangling bonds and defects, making them easier to integrate with other materials. A clean interface is a prerequisite for materials to maintain their intrinsic properties after integration with 2D FE materials, and this is key to achieving controllable and excellent performance in electronic devices [22]. In addition, compared to the insulating properties of traditional perovskite ferroelectrics, 2D FE materials are usually semiconductors with good carrier mobilities, making them suitable for use as channel materials in FET. A new type of electronic device, ferroelectric semiconductor field-effect transistor (FeS-FET), has been fabricated based on such properties [23,24], providing new opportunities for solving charge-trapping problems at semiconductor/dielectric interfaces in traditional FeFETs, as well as related in-memory computing. Furthermore, some novel properties have also been observed in 2D FE materials and their bulk counterparts (bulk vdW FEs). For example, bulk and multilayer $CuInP_2S_6$ exhibit a unique quadruple-well potential [25], which has never been observed in traditional perovskite FEs. Coupling between 5*d* electron-induced spin-orbital coupling (SOC) and ferroelectricity has been predicted to emerge in layered perovskite FEs Bi_2WO_6 [26], enabling control of spin texture through reversal of FE polarization.

The field of 2D FE materials is still in its early stages of development, motivating researchers to discover and design more 2D FE materials with excellent properties. Advances in high-performance computing and theoretical methods have made density functional theory (DFT) calculations, high-throughput calculations, and machine learning powerful tools for material design [27–31]. To date, tens of new 2D FE materials have been theoretically predicted, offering a wealth of candidates for experimental fabrication. This review presents recent progress in the theoretical prediction of 2D FE materials and summarizes the strategies for their design. Readers interested in the fabrication, properties, and related devices are encouraged to refer to previous reviews in the field [32–37]. In the following, we begin with a short summary of the currently fabricated and predicted 2D FE materials, and then focus on the strategies for designing 2D FE materials. Finally, we provide a perspective on the development of 2D FE materials and summarize the existing challenges.

2. Currently fabricated and predicted 2D FEs

This section provides a short summary of the 2D FE materials that have been reported to date before we discuss their theoretical design strategies. Currently, there are tens of 2D FE materials that have been either experimentally fabricated or theoretically predicted. Some of these 2D FE materials possess the same prototype structure but different chemical elements (e.g., $CuInP_2S_6$ and $CuCrP_2S_6$), which can be viewed as the same material family. Here summarize eight different types of 2D FE material families, as shown in Table 1. Each 2D FE family is named after a representative material in the group and the corresponding structure prototypes are depicted in Fig. 1. It is worth noting that while these eight families cover a significant majority of the 2D FE materials reported so far, there are still some single cases, such as functionalized graphene, bismuth oxychalcogenides, and 2D magnetoelectric multiferroics, that are not included. For further information on these materials, readers may refer to the references [38–44].

3. Strategy-I: designing new 2D FEs under a given structure prototype

The most notable characteristic of FE materials is spontaneous polarization, which requires the structure of ferroelectric materials to be non-centrosymmetric to achieve the separation of positive and negative charge centers. In addition, the polarizations of FE materials must be (readily) switchable, which is the key difference between FE and polar materials. Thus, the following criteria must be met when designing 2D FE materials theoretically:

(i) The designed materials should be able to retain stable non-centrosymmetric structures.

(ii) The non-centrosymmetric structure should be the ground state of the designed materials.

(iii) There should be a transition path that allows the FE polarization to be readily switched.

In actual practice, the stability of the designed materials can be evaluated preliminarily by checking whether the initial structure is maintained after structural relaxation, and the dynamic stability can then be further evaluated by checking the presence of soft modes in the phonon dispersions. The thermal stability of the designed materials can be evaluated by checking their structural evolution under certain temperature molecular dynamics simulations. The ground states of the designed materials can be identified by comparing the energy difference between the centrosymmetric (paraelectric (PE) phase) and non-centrosymmetric (FE phase) structures. The ferroelectric switching barrier and path can be calculated using the nudged elastic-band (NEB) method. The magnitude of polarization is most commonly determined using the Berry phase method (modern theory of polarization) [73–76]. For 2D FE materials with out-of-plane polarization, the polarization can also be calculated by integrating ρz along the z-direction owing to the existence of vacuum in the unit cell, where ρ is the local charge density (containing both ionic and electronic contributions), and z is the coordinate along the out-of-plane polarization. Additionally, the electronic properties of the designed materials should also be investigated. Generally, FE materials are either insulating or semiconducting because, in principle, the conduction electrons in metals screen out the internal electric field arising from the FE polarization. Recently, however, both bulk and 2D FE metals have been experimentally discovered [65,77,78], indicating the possibility of metallic FE materials. However, the mechanism of the coexistence of ferroelectricity and metallicity should be investigated further to provide a deeper understanding. Investigation of the electronic properties of the designed 2D FE materials will also provide guidelines for the design of related functional devices.

Given the above general framework, the most intuitive way to design 2D FE materials is to use the structure of an experimentally fabricated 2D FE material as a prototype and then design new 2D FE materials by trying different combinations of chemical elements. It is noted that a large number of materials can be generated owing to different combinations of chemical elements; thus, high-throughput calculations and machine learning methods are usually employed to facilitate the screening of sTable 2D FE materials. For example, in 2020, a group of 2D FE materials, $M_IM_{II}P_2\times_6$ (M_I, M_{II} = two kinds of metal atoms, X = O, S, Se, Te), was theoretically predicted using machine learning methods [47]. The workflow of the screening process is illustrated in Fig. 2a. Beginning with the structural prototype of 2D FE $CuInP_2S_6$, 2964 different types of 2D FE materials were generated through different combinations of chemical elements. Primarily, 605 of the 2964 materials were selected, and the FE materials were identified by simply evaluating the vertical displacement of metal atoms. Then, 605 selected materials were employed as the training dataset to train the machine learning model. The precision of the machine-learning model was evaluated by comparing the DFT and machine-learning results. To improve precision,

Table 1
Families of 2D FE materials that are reported currently (experimentally fabricated or theoretically predicted). For the abbreviation in the table, "Y" represents one or more 2D FE materials belonging to the materials family have been fabricated; "OOP" and "IP" represent "out-of-plane polarization" and "in-plane polarization", respectively; "exp" and "th" represent experimental and theoretical results, respectively. AFE represents antiferroelectric.

Materials family	Fabricated?	Polarization direction	Thinnest thickness	Refs.
$CuInP_2S_6$ type	Y	OOP	4 nm (exp)	[21,45–49]
SnTe type	Y	IP	0.63 nm (exp)	[20,50]
α-In_2Se_3 type	Y	OOP & IP	2 nm (exp)	[51–56]
β'-In_2Se_3 type	Y	IP (AFE)	1.05 nm (exp)	[57,58]
d1T-$MoTe_2$ type	Y	OOP	0.8 nm (exp)	[59,60]
Sliding ferroelectrics	Y	OOP	bilayer, ~0.3 nm (exp)	[61–66]
Sc_2CO_2 type (functionalized MXene)	N	OOP	monolayer (th)	[67,68]
$Hf_2Ge_2S_6$ type	N	OOP	monolayer (th)	[69–71]

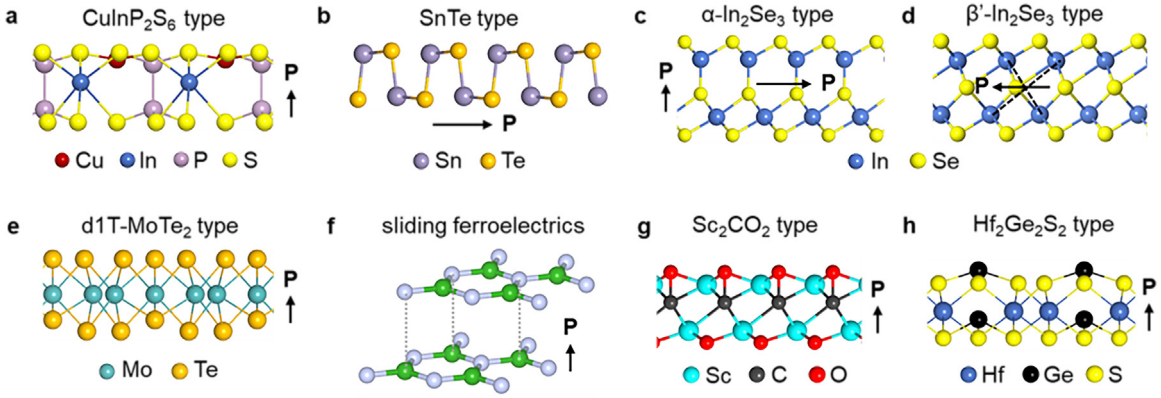

Fig. 1. Structure prototypes of the eight 2D FE materials families shown in Table 1. Polarization directions are shown by the black arrow. For sliding ferroelectrics, we take AB-stacked bilayer h-BN as an example to show their structures and polarization directions. The structure prototypes are replotted according to the structure reported in [20,21,52,59,61,67,69,72].

293 additional materials were added to the training dataset during the training process. The remaining 2066 materials were classified using a trained machine-learning model. Finally, the stability and properties of the screened materials were investigated in detail. A total of 44 2D FE semiconductors and 16 2D FE metals were identified through DFT calculations.

For the predicted 2D FE metal, the mechanism of the coexistence of ferroelectricity and metallicity was further understood by investigating the spatial charge distribution. The left panel of Fig. 2b, c show the partial charge densities in the range of $|E-E_F|< 0.05eV$ (E_F is the Fermi level) of the two predicted 2D FE metals $InZrP_2Te_6$ and $AuZrP_2S_6$. Because the conducting electrons are mainly contributed by the electronic state near the Fermi level, these results indicate that the conducting electrons of the predicted 2D FE metals are mainly located on the upper surface of the materials. The reduced conducting electron densities, defined as $\iint \rho_c(\vec{r})dxdy$, where $\rho_c(\vec{r})$ is the conducting electron density, are represented by the blue line in the right panel of Fig. 2b, c. The reduced charge density difference between the FE and PE phases $\iint[\rho_{FE}(\vec{r}) - \rho_{PE}(\vec{r})]dxdy$), which reflects the densities of the electrons contributing to the polarization, is shown using the red dashed line in the right panel of Fig. 2b, c. This demonstrates the spatial separation of the conducting electrons and electrons contributing to polarization. Moreover, the conducting electrons in $InZrP_2Te_6$ and $AuZrP_2S_6$ were mainly contributed by atoms exhibiting no (or very less) displacement (see Fig. 3 of Ref. [47] for details), which is consistent with the "decoupled electron mechanism" proposed by Puggioni and Rondinelli [79–81]. These results provide clues for understanding the coexistence of ferroelectricity and metallicity in predicted 2D FE metals.

Abundant new 2D FE materials can be predicted by exploring various chemical element combinations under a given structure prototype. Moreover, such a strategy provides guidelines for identifying specific 2D FE materials for FE functional device fabrication. A recent experimental technique, heteroatoms intercalation, has enabled the fabrication of functional devices by inserting functional materials into the graphene/metal interface [82–87]. For example, rectification and tunneling devices were made by intercalating silicene and SiO_2 into a graphene/Ru interface [84,87]. It is desirable to fabricate FE functional devices using the intercalation technique because the performance of FE functional devices highly depends on the interface conditions [22,88], while the introduction of contaminations is avoided in such a technique benefiting from the elimination of the transfer process. Motivated by the above considerations, the feasibility of fabricating FE functional devices by intercalating 2D FE materials into the graphene/Ru interface was theoretically investigated [56]. Monolayer α-In_2Se_3, which is also referred to as QL-In_2Se_3 (a monolayer In_2Se_3 containing quintuple atomic layers), has the potential to be a promising candidate for intercalation because it contains few chemical elements. However, it was found that QL-In_2Se_3 loses its ferroelectricity once intercalated into the graphene/Ru interface owing to the strong bonding between QL-In_2Se_3 and Ru, as shown in Fig. 3a, d. Given that SiO_2 was successfully intercalated into the graphene/Ru interface and that the intercalated SiO_2 is weakly bonded to Ru, an alternative method is to intercalate 2D FE metal oxide into the graphene/Ru interface. Based on the above considerations, two types of 2D metal oxides, QL-M_2O_3 (M=Al, Y), were identified as stable FEs. Moreover, it is proved that QL-M_2O_3 (M=Al, Y) maintains ferroelectricity after intercalation into the graphene/Ru interface, as reflected by the electrostatic potential drop in Fig. 3e, f (only the case of QL-Al_2O_3 is shown as an example).

The electronic properties of the graphene/QL-M_2O_3/Ru heterostructures were further investigated to provide guidelines for the design of functional devices. Herein, the case of QL-Al_2O_3 is considered as

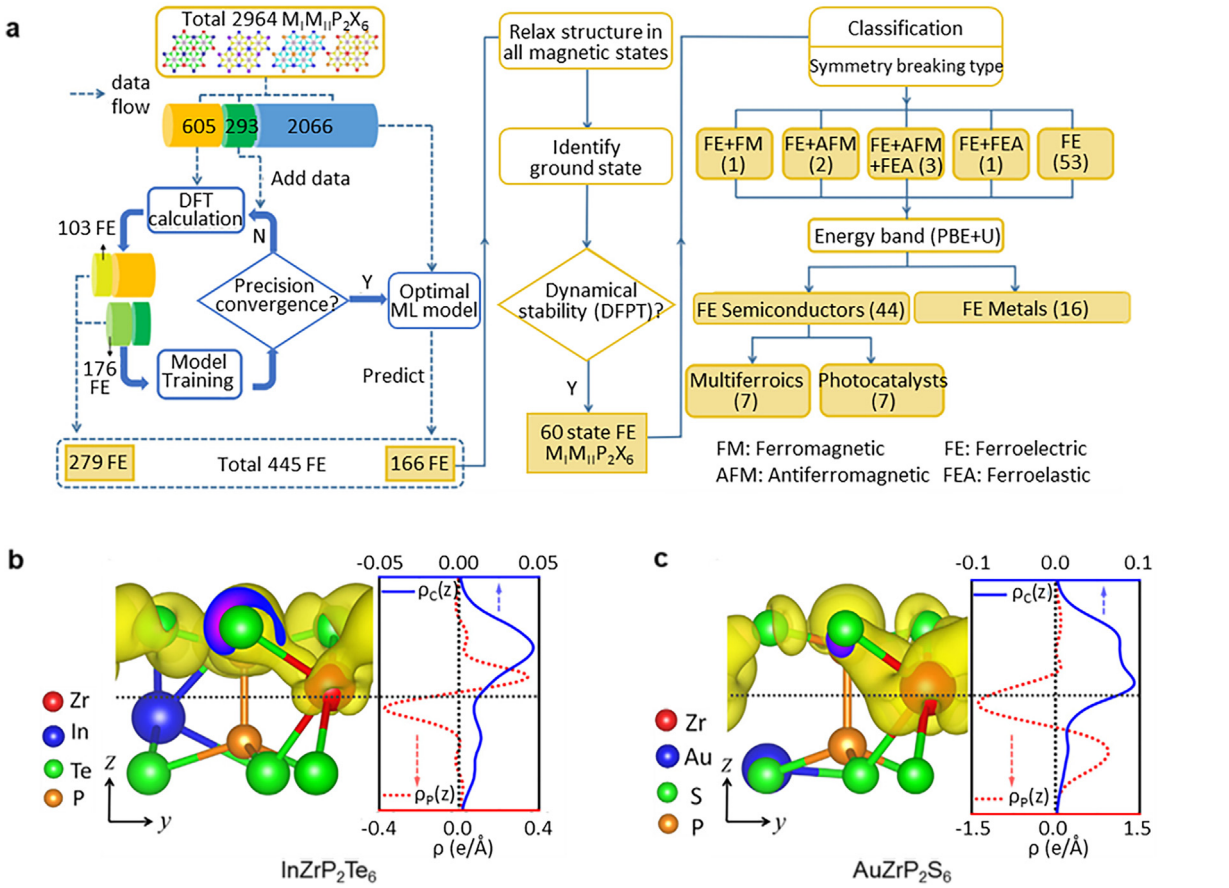

Fig. 2. Theoretical prediction of the 2D FE materials family $M_IM_{II}P_2\times_6$. (a) Workflow of the screening process of 2D FE $M_IM_{II}P_2\times_6$. (b), (c) Partial charge density of the two predicted 2D FE metals $InZrP_2Te_6$ and $AuZrP_2S_6$. The energy range of the partial charge is $|E-E_F|< 0.5$eV. Right panel: reduced conducting electron density (blue line) and reduced "FE–PE electron density difference" (red dashed line) of $InZrP_2Te_6$ and $AuZrP_2S_6$ [47].

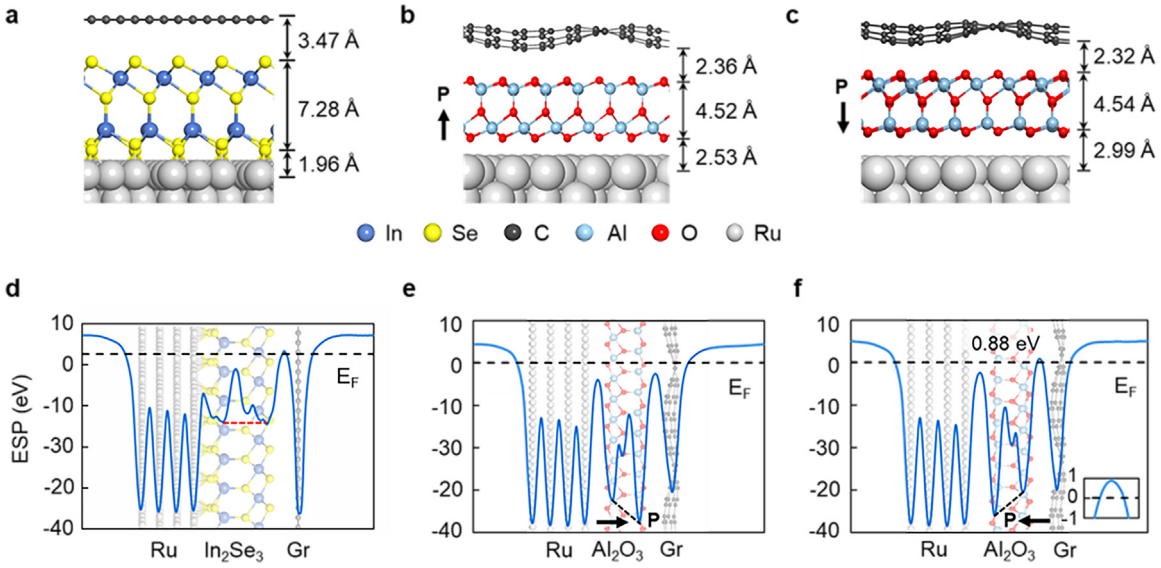

Fig. 3. Ferroelectricity of QL-In_2Se_3 and QL-Al_2O_3 in the graphene/QL-In_2Se_3(Al_2O_3)/Ru heterostructure [56]. (a)-(c) Relaxed structure of graphene/QL-In_2Se_3(Al_2O_3)/Ru heterostructures, where the polarization of QL-Al_2O_3 points towards and away from graphene in (b) and (c), respectively. (d)-(f) Plane-averaged electrostatic potential (ESP) of graphene/QL-In_2Se_3(Al_2O_3)/Ru heterostructures.

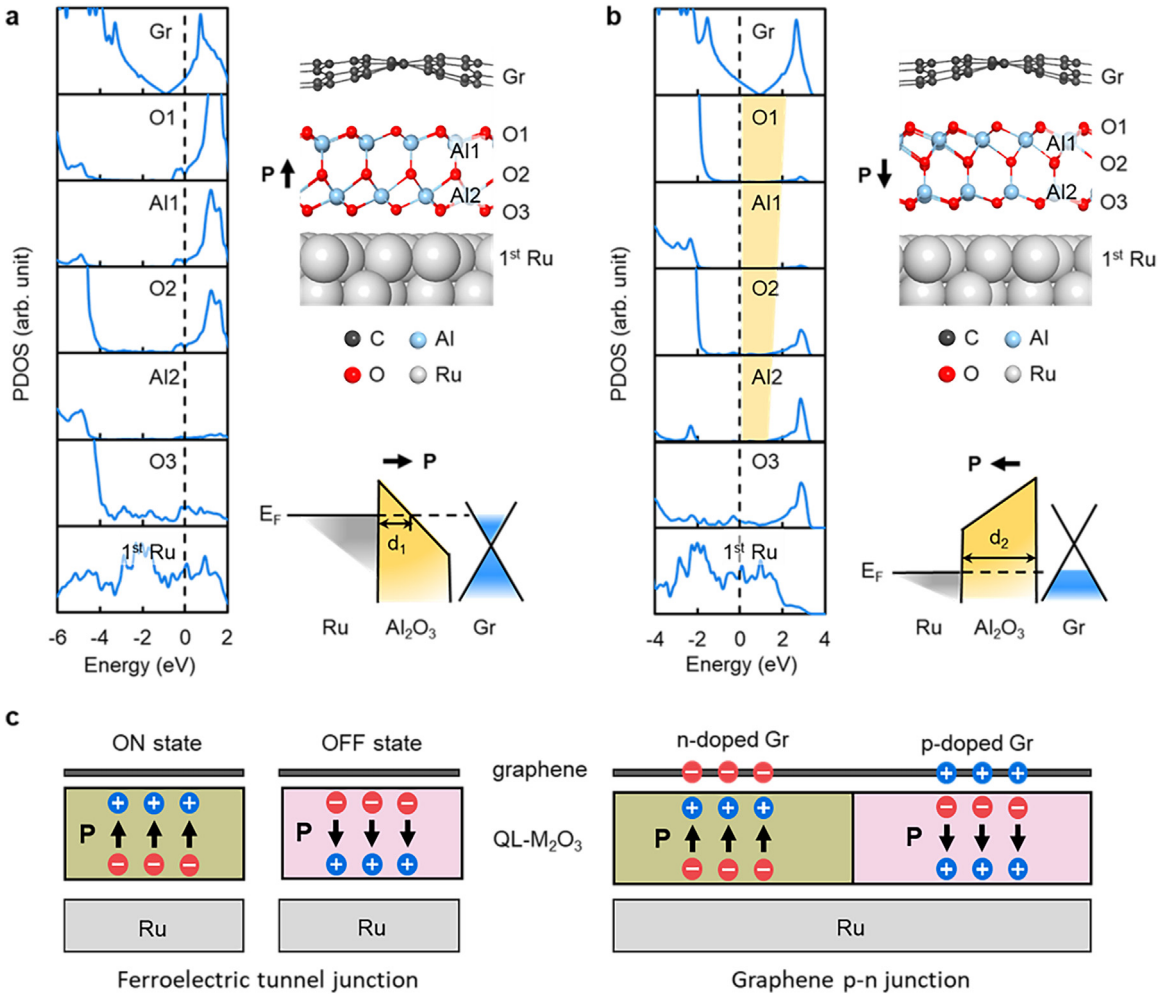

Fig. 4. Possible FE functional devices based on graphene/QL-Al_2O_3/Ru heterostructure [56]. (a),(b) Layered-resolved projected density of states of graphene/QL-Al_2O_3/Ru heterostructure, where the polarization points towards and backwards graphene, respectively. (c) Schematic of two kinds of FE functional devices based on graphene/QL-Al_2O_3/Ru heterostructure.

an example to demonstrate. The layer-resolved projected density of states (PDOS) of the graphene/QL-Al_2O_3/Ru heterostructure is shown in Fig. 4a, b, where the polarization points towards and away from graphene, respectively. As shown in Fig. 4a, when the polarization points towards graphene near the graphene/QL-Al_2O_3 interface, the conduction band of QL-Al_2O_3 is located below the Fermi level, and the heterostructure is conductive. However, when the polarization points backwards to graphene, a tunneling barrier forms near the graphene/QL-Al_2O_3 interface, as shown by the yellow region in the layer-resolved PDOS in Fig. 4b. Enabled by the polarization modulation of the barrier width, the resistive state of the graphene/QL-Al_2O_3/Ru heterostructure can be modulated by the polarization direction, whereby the graphene/QL-Al_2O_3/Ru can function as an FTJ, shown schematically in the left panel of Fig. 4c. Moreover, the doping type of graphene in the heterostructure is also modulated by the polarization direction, as shown by the PDOS of graphene in Fig. 4a and b. Thus, based on the graphene/QL-Al_2O_3/Ru heterostructure, the core part of the graphene photodetector, graphene p-n junction, can be fabricated by poling the adjacent QL-Al_2O_3 domain in a different polarization direction, as shown by the schematic in the right panel of Fig. 4c.

In summary, designing 2D FEs under a given structure prototype using different chemical element combinations provides an intuitive way to discover new 2D FEs as well as guidelines for the design of related FE functional devices.

4. Strategy-II: design new 2D FEs by designing new 2D FE structure prototype

Designing new 2D FEs under a known prototype structure provides an effective way to discover new 2D FEs. However, limited by the preliminarily given structure prototype, it is challenging to discover new 2D FE materials whose atomic configurations have not yet been explored by such a strategy. An alternative strategy to design new 2D FE materials is to begin with the design of a new 2D FE structure prototype, and then search for materials that are stable under the designed structure prototypes. The limitation imposed by the rare amount of 2D FE structure prototypes is lifted in such a strategy. Moreover, according to the structure-property relationship, the new structural prototype provides possibilities for the discovery of new properties.

Investigating the soft phonon mode (phonon mode with an imaginary frequency) of 2D materials may provide insight into designing new 2D FE structure prototypes. It is well known that, for some perovskite ferroelectrics, the paraelectric-to-ferroelectric phase transition is driven by soft-mode-induced structural distortion. In some cases, this scenario holds true for 2D materials as well. For example, the ground state of monolayer MoS_2 exhibits a 2H structure. The 1T structure of MoS_2, as shown in Fig. 5a, is not stable, as reflected by the soft mode near the K-point in the phonon dispersion (Fig. 5e). The vibration mode corresponding to the imaginary frequency at the K-point is indicated by the green arrows in Fig. 5b, involving the in-plane displacement of the Mo

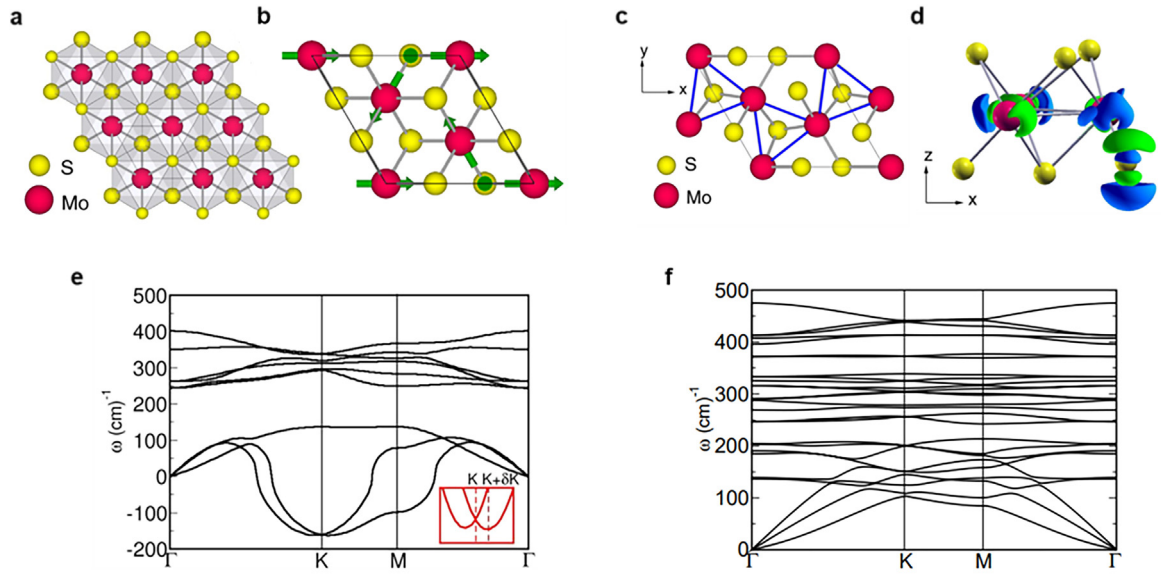

Fig. 5. Prediction of 2D FE d1T-MoS_2 monolayer [60]. (a) Structure of 1T-MoS_2 monolayer. (b) Vibration mode of the imaginary frequency of 1T-MoS_2 at K-point. (c) Structure of d1T-MoS_2 monolayer. (d) The electron density difference between 1T-MoS_2 and d1T-MoS_2 monolayer. (e),(f) Phonon dispersions of 1T-MoS_2 and d1T-MoS_2, respectively.

atoms and the vertical displacement of the S atoms. Driven by the soft mode, a new monolayer MoS_2 structure featuring trimerized Mo atoms (marked by blue triangles in Fig. 5c) forms, which is referred to as distorted 1T (d1T)-MoS_2. The phonon dispersion of the d1T-MoS_2 monolayer is shown in Fig. 5f. The absence of the soft mode indicates that the d1T-MoS_2 structure was stable. Furthermore, the centrosymmetry of the original 1T-MoS_2 structure was broken by the vertical displacement of the S atoms, inducing out-of-plane polarization. The charge density difference between d1T-MoS_2 and 1T-MoS_2 is spatially asymmetric along the z-direction (Fig. 5d), further proving the existence of out-of-plane polarization. Based on the above evidences, the d1T-MoS_2 monolayer was predicted to be a 2D FE material in 2014 [60]. Subsequently, d1T-$MoTe_2$ was successfully fabricated in 2019. Moreover, it was experimentally verified that d1T-$MoTe_2$ was still able to maintain ferroelectricity when its thickness was reduced to the monolayer limit, which is the thinnest of the experimentally reported 2D FEs with out-of-plane polarization [59].

In addition to investigating the soft phonon mode, exploring 2D materials exhibiting ion-transport-like behavior may also provide insights into the prediction of 2D FE materials with a new structure prototype. The displacement of ions is the source of ferroelectricity in most FE materials, and the ion transport-like behavior offers the potential to induce such displacement and thus ferroelectricity. For example, one of the most well-known 2D FE materials, $CuInP_2S_6$, demonstrates both ferroelectricity originating from the displacement of Cu atoms and Cu ion transport properties [45]. Another example is the theoretical prediction of the 2D FE material family M_2 (Ge, Sn)$_2Y_6$. One of the recently discovered 2D ferromagnetic materials, $Gr_2Ge_2Te_6$ [89–91], exhibits Ge atom interlayer flipping behavior under high-pressure [92,93] and during the amorphous $Cr_2Ge_2Te_6$ crystalline process [94]. This indicates the possibility of inducing ferroelectricity in $Cr_2Ge_2Te_6$-like structures through Ge atom displacement. Beginning with the centrosymmetric $Cr_2Ge_2Te_6$-like structure (denoted as $M_2{\times}_2Y_6$), a new 2D FE structure $M_2{\times}_2Y_6$ is generated by inducing X-dimer displacement, where M are metal atoms, X are Si, Ge, Sn atoms, Y are S, Se, Te atoms. Using high-throughput calculations, 16 $M_2Ge_2Y_6$ and 28 $M_2Sn_2Y_6$ monolayers were identified as sTable 2D FEs. Among the predicted 2D FE $M_2{\times}_2Y_6$ layers, eight were predicted to be potential 2D FE metals, such as $Pd_2Ge_2Te_6$ and $Os_2Sn_2S_6$. All of these materials contain 5*d* transition metal elements, suggesting a connection between metallicity in the FE $M_2{\times}_2Y_6$ layer and the presence of 5*d* electrons. However, this hypothesis requires further verification. The details of these materials are documented in Ref. [69,95].

The formation mechanism of the 2D FE $M_2{\times}_2Y_6$ monolayer can be further understood by investigating the phonon dispersions of $M_2{\times}_2Y_6$. Here, one of the identified 2D FEs, $Hf_2Ge_2Te_6$, is considered as an example to demonstrate. The structure and phonon dispersion of $Hf_2Ge_2Te_6$ in the centrosymmetric phase (denoted as centrosymmetric I, short for C1) are shown in Fig. 6a and d, respectively. Clearly, an optical phonon band with an imaginary frequency emerges in the phonon dispersion of the C1 phase $Hf_2Ge_2Te_6$ monolayer, thereby indicating that the C1 phase is not stable. The vibration mode of the imaginary frequency at the Γ-point is shown in Fig. 6g, mainly owing to the vertical displacement of the Ge dimer. This soft mode breaks the centrosymmetry of the C1 phase, resulting in the formation of the FE phase. The structure and phonon dispersion of the $Hf_2Ge_2Te_6$ monolayer in the FE phase are shown in Fig. 6b and e, respectively. The absence of an imaginary frequency proves the dynamic stability of the FE $Hf_2Ge_2Te_6$ monolayer.

Additionally, flat phonon bands were observed in the phonon dispersion of the FE $Hf_2Ge_2Te_6$ monolayer. Generally, the vibration modes of the flat phonon band are localized and thus can be activated independently, and this may cause the emergence of a new phase in the $Hf_2Ge_2Te_6$ monolayer. Based on these considerations, the vibration modes of one of the flat phonon bands (marked by blue) at the K- and Γ-points were investigated, as shown in Fig. 6h, i, which tend to separate the two Ge atoms in the Ge dimer. These vibrational modes indicate the emergence of another centrosymmetric phase of $Hf_2Ge_2Te_6$ (denoted as centrosymmetric-II, short for C2), where the two Ge atoms are located at the upper and lower surfaces of $Hf_2Ge_2Te_6$ and are mirror-symmetric relative to the M atom plane. Such a structure is dynamically stable (Fig. 6f), but has a higher energy than the FE phase, which is the metastable phase of the $Hf_2Ge_2Te_6$ monolayer. The existence of the C2 phase enables two possible FE switching paths: FE-up→C1(C2)→FE-down. Details of these two paths can be found in Ref. [69]. More interestingly, it has been predicted that HfO_2 exhibits flat phonon band-induced scale-free ferroelectricity, featuring independently switchable polarization in an adjacent unit cell [96]. Such characteristics are also predicted to emerge in the FE $Hf_2Ge_2Y_6$ (Y = S, Se, Te) monolayer (Fig. 6j), mak-

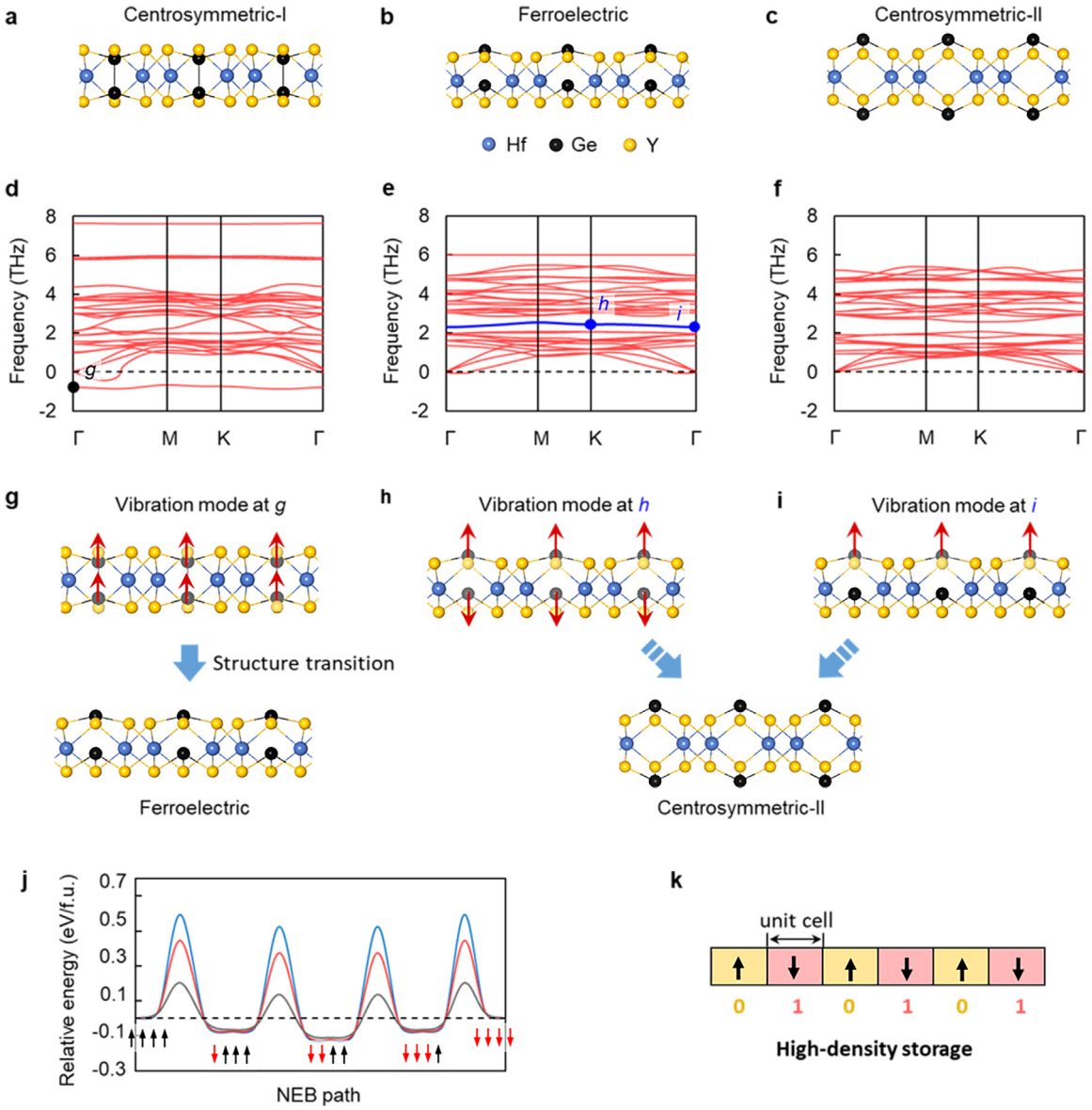

Fig. 6. Formation mechanism of ferroelectricity in $M_2\times_2Y_6$ and its novel properties [69]. (a)-(c) Structure of $Hf_2Ge_2Te_6$ monolayer in centrosymmetric-I, ferroelectric and centrosymmetric-II phases, respectively. (d)-(f) Phonon dispersions of $Hf_2Ge_2Te_6$ monolayer in centrosymmetric-I, ferroelectric and centrosymmetric-II phases, respectively. (g)-(i) Vibration modes of the points marked in (d)-(e), and the schematic of the formation of ferroelectric and centrosymmetric-II phase. Red arrows represent the displacement of Ge atoms. (j) Ferroelectric switching barrier of $Hf_2Ge_2Y_6$ from uniformed polarization-up state ↑↑↑↑ to uniformed polarization-down state ↓↓↓↓. Each barrier corresponds to the polarization reversal in one unit-cell. (k) Schematic of a high-density storage device based on ferroelectric $M_2\times_2Y_6$ monolayer.

ing it promising for applications involving high-density storage, where the size of the memory unit can shrink to a one-unit-cell length (Fig. 6k).

Designing new 2D FE structure prototypes provides an alternative way to design new 2D FE materials, which overcomes the limitations imposed by known 2D FE structure prototypes. Moreover, this strategy provides fresh opportunities to discover new properties associated with new structures.

5. Strategy-III: design new 2D FEs through stacking engineering

The previous two strategies focus on designing intrinsic 2D FE materials, meaning those that possess an inherent non-centrosymmetric structure. Most 2D materials have a centrosymmetric atomic configuration, which precludes the possibility of ferroelectricity in their monolayer form. Stacking engineering provides an opportunity to design new 2D FE materials. Generally, when 2D layers containing binary or more chemical compounds are stacked in a bilayer form, the local atomic configurations of the top and bottom layers are inequivalent at some specific stacking modes. Such inequivalence induces interlayer charge transfer and subsequent out-of-plane polarization. An example is bilayer h-BN. In 2017, it was predicted that AB-stacked bilayer h-BN is a 2D FE material with out-of-plane polarization [63]. Lately in 2021, such theoretical predictions were verified experimentally [61,62]. The key to inducing ferroelectricity is the stacking mode. For bilayer h-BN, the most stable stacking mode is AA' stacking, where the B(N) atoms in the upper layer were located above the N(B) atoms in the lower layer, as shown in Fig. 7a. Such a stacking mode maintains inversion symmetry and, thus, cannot be ferroelectric. Another metastable stacking mode of h-BN is AB stacking, while the energy difference between AA' and AB stacking is very little [97–99], thus AB-stacked bilayer h-BN is also observed in experiments. In the AB stacking mode, the B atoms in the upper layer are located above the N atoms in the lower layer, whereas the N atoms

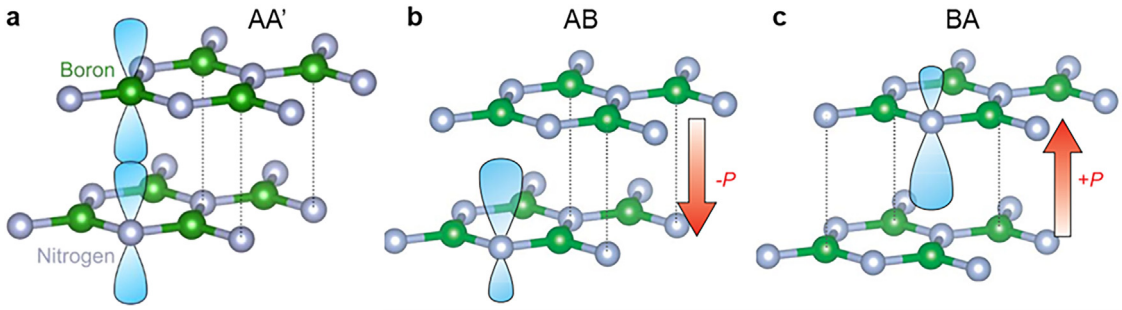

Fig. 7. Schematic of the AA' AB and BA stacking mode of bilayer h-BN, as well as the polarization in AB- and BA-stacked bilayer h-BN [61].

in the upper layer are located at the empty site of the hexagon ring of the lower layer. Such an atomic arrangement causes distortion of the N orbitals, thus inducing polarization in AB-stacked h-BN. By interlayer sliding, AB-stacking can be transformed into BA-stacking to achieve polarization reversal. Featured by the interlayer sliding enabled polarization switching, such materials are named as sliding ferroelectrics. Bilayer 1T'-WTe_2, InSe, AlN and ZnO etc., have also been predicted to be sliding ferroelectrics [63,64,66].

6. Summary and outlook

The miniaturization of electronic devices has sparked significant research interest in ferroelectric (FE) thin films. As traditional perovskite FEs usually suffer from polarization instability below a certain critical thickness, the discovery of 2D FE materials provides other opportunities. To date, several kinds of 2D FE materials have been fabricated experimentally, and it has been proven that they can preserve the FE polarization when their thickness is reduced to a few nanometers or to the monolayer limit. Additionally, 2D FE materials exhibit properties that are not found in traditional bulk ferroelectrics, such as clean interfaces, insensitivity to substrate selection, and good mobility as a semiconductor, making them promising for use in new FE functional devices. Marked by the experimental discovery of 2D FE materials in 2016, research on 2D FE materials is still in its first decade. This field is rapidly advancing and there is still much room for exploration. In this review, we discuss the recent progress in the theoretical design of 2D FE materials and summarize some strategies for the design of 2D FE materials The goal is to provide guidelines for the theoretical prediction of 2D FE materials and inspire future research in this field. The following are some possible directions for future research on 2D FE materials.

(i) Theoretical design of 2D FE materials with large polarizations, semiconducting properties, and a new structure prototype. To date, 2D FE candidates have been limited. The theoretical prediction of 2D FE materials with the facilitation of high-throughput calculations and machine learning methods remains desirable. Certain properties should be noted during the design process. The first is the magnitude of polarization. Currently, the most prominent obstacle for 2D FE materials is that their polarizations are much smaller than those of traditional perovskite FEs. The design of 2D FE materials with a large polarization and the investigation of the mechanism to enhance the polarization of 2D FE materials is highly desired from both application and fundamental research perspectives. In addition, the design of 2D FE semiconductors with large carrier mobility will provide candidates for new types of FE functional devices. Based on the structure–property relationship, the design of 2D FE materials with new structures may provide opportunities for overcoming these problems.

(ii) Coupling between FE ordering and other properties, for example, ferromagnetic (FM) orderings, valley degrees, spin-orbital coupling (SOC), and topological properties. Such coupling may provide opportunities for the design of new functional devices. For example, with respect to 2D systems, coupling between FE and FM orderings can be achieved in single phase magnetoelectric multiferroics [41–44] or FE/FM heterostructure [100–106], enabling the electric control of magnetic properties, thus are highly-desired in spintronics. Coupling between FE polarization and valley degree of freedom provides platform to realize polarizer driven by electrical means [107]. Coupling between FE polarization and SOC motivate the research on 2D ferroelectric SOC semiconductor, a kind of functional materials enabling electrical control of spin texture [108,109]. Materials containing 5*d* electrons are suitable candidates for studying the coupling between FE ordering and SOC because strong SOC can be expected in such materials. Nonvolatile control of topological states, for example, polarization control of the transformation between topological and non-trial states, can also be realized in 2D systems where FE ordering and topological states are coupled [110,111].

(iii) Domain dynamics of 2D FE materials. The FE domain is a crucial storage unit for FE-based memory devices and the size and properties of the FE domain affect the performance of these devices, such as their response to external strain and electric fields. Currently, studies on the domain of 2D FE materials are limited and this area is ripe for further research. Theoretical studies at different scales can be carried out using DFT calculations, *ab initio* and classical molecular dynamics simulations, and phase-field simulations.

Declaration of competing interest

The authors declare that they have no conflicts of interest in this work.

Acknowledgments

We acknowledge financial support from National Natural Science Foundation of China (52250402 and 61888102), Strategic Priority Research Program of the Chinese Academy of Sciences (XDB30000000 and XDB28000000), CAS Project for Young Scientists in Basic Research (YSBR-003), and the Fundamental Research Funds for the Central Universities.

References

[1] J. Valasek, Piezo-electric and allied phenomena in rochelle salt, Phys. Rev. 17 (4) (1921) 475–481.
[2] V. Garcia, M. Bibes, Ferroelectric tunnel junctions for information storage and processing, Nat. Commun. 5 (1) (2014) 4289.
[3] Z. Wen, D. Wu, Ferroelectric tunnel junctions: modulations on the potential barrier, Adv. Mater. 32 (27) (2020) 1904123.
[4] J.Y. Kim, M.J. Choi, H.W. Jang, Ferroelectric field effect transistors: progress and perspective, APL Mater. 9 (2) (2021) 021102.
[5] C.R. Bowen, H.A. Kim, P.M. Weaver, S. Dunn, Piezoelectric and ferroelectric materials and structures for energy harvesting applications, Energy Environ. Sci. 7 (1) (2014) 25–44.
[6] C. Paillard, X. Bai, I.C. Infante, et al., Photovoltaics with ferroelectrics: current status and beyond, Adv. Mater. 28 (26) (2016) 5153–5168.
[7] J. Junquera, P. Ghosez, Critical thickness for ferroelectricity in perovskite ultrathin films, Nature 422 (6931) (2003) 506–509.

[8] C.H. Ahn, K.M. Rabe, J.M. Triscone, Ferroelectricity at the nanoscale: local polarization in oxide thin films and heterostructures, Science 303 (5657) (2004) 488–491.
[9] M. Dawber, K.M. Rabe, J.F. Scott, Physics of thin-film ferroelectric oxides, Rev. Mod. Phys. 77 (4) (2005) 1083–1130.
[10] D.D. Fong, G.B. Stephenson, S.K. Streiffer, et al., Ferroelectricity in ultrathin perovskite films, Science 304 (5677) (2004) 1650–1653.
[11] Z. Xi, J. Ruan, C. Li, et al., Giant tunnelling electroresistance in metal/ferroelectric/semiconductor tunnel junctions by engineering the Schottky barrier, Nat. Commun. 8 (1) (2017) 15217.
[12] H. Wang, Z.R. Liu, H.Y. Yoong, et al., Direct observation of room-temperature out-of-plane ferroelectricity and tunneling electroresistance at the two-dimensional limit, Nat. Commun. 9 (1) (2018) 3319.
[13] D. Ji, S. Cai, T.R. Paudel, et al., Freestanding crystalline oxide perovskites down to the monolayer limit, Nature 570 (7759) (2019) 87–90.
[14] K.S. Novoselov, A.K. Geim, S.V. Morozov, et al., Electric field effect in atomically thin carbon films, Science 306 (5696) (2004) 666–669.
[15] G. Giovannetti, P.A. Khomyakov, G. Brocks, et al., Substrate-induced band gap in graphene on hexagonal boron nitride: *ab initio* density functional calculations, Phys. Rev. B 76 (7) (2007) 073103.
[16] K.F. Mak, C. Lee, J. Hone, et al., Atomically thin MoS_2: a new direct-gap semiconductor, Phys. Rev. Lett. 105 (13) (2010) 136805.
[17] G.R. Bhimanapati, Z. Lin, V. Meunier, et al., Recent advances in two-dimensional materials beyond graphene, ACS Nano 9 (12) (2015) 11509–11539.
[18] Y.T. Zhang, Y.P. Wang, X. Zhang, et al., Structure of amorphous two-dimensional materials: elemental monolayer amorphous carbon versus binary monolayer amorphous boron nitride, Nano Lett. 22 (19) (2022) 8018–8024.
[19] X.L. Zhang, D.L. Bao, W.H. Dong, et al., Anisotropic high carrier mobilities of one-third-hydrogenated group-v elemental monolayers, J. Phys. Chem. C 124 (23) (2020) 12628–12635.
[20] K. Chang, J. Liu, H. Lin, et al., Discovery of robust in-plane ferroelectricity in atomic-thick SnTe, Science 353 (6296) (2016) 274–278.
[21] F. Liu, L. You, K.L. Seyler, et al., Room-temperature ferroelectricity in $CuInP_2S_6$ ultrathin flakes, Nat. Commun. 7 (1) (2016) 12357.
[22] J. Wu, H.Y. Chen, N. Yang, et al., High tunnelling electroresistance in a ferroelectric van der Waals heterojunction via giant barrier height modulation, Nat. Electron. 3 (8) (2020) 466–472.
[23] M. Si, A.K. Saha, S. Gao, et al., A ferroelectric semiconductor field-effect transistor, Nat. Electron. 2 (12) (2019) 580–586.
[24] S. Wang, L. Liu, L. Gan, et al., Two-dimensional ferroelectric channel transistors integrating ultra-fast memory and neural computing, Nat. Commun. 12 (1) (2021) 53.
[25] J.A. Brehm, S.M. Neumayer, L. Tao, et al., Tunable quadruple-well ferroelectric van der Waals crystals, Nat. Mater. 19 (1) (2020) 43–48.
[26] H. Djani, A.C. Garcia-Castro, W.Y. Tong, et al., Rationalizing and engineering Rashba spin-splitting in ferroelectric oxides, NPJ Quant. Mater. 4 (1) (2019) 51.
[27] S. Curtarolo, G.L.W. Hart, M.B. Nardelli, et al., The high-throughput highway to computational materials design, Nat. Mater. 12 (3) (2013) 191–201.
[28] J. Wei, X. Chu, X.Y. Sun, et al., Machine learning in materials science, InfoMat 1 (3) (2019) 338–358.
[29] Y. Iwasaki, M. Ishida, M. Shirane, Predicting material properties by integrating high-throughput experiments, high-throughput *ab-initio* calculations, and machine learning, Sci. Technol. Adv. Mater. 21 (1) (2020) 25–28.
[30] K. Choudhary, K.F. Garrity, V. Sharma, et al., High-throughput density functional perturbation theory and machine learning predictions of infrared, piezoelectric, and dielectric responses, NPJ Comput. Mater. 6 (1) (2020) 64.
[31] X.L. Zhang, J. Pan, X. Jin, et al., Database construction for two-dimensional material-substrate interfaces, Chin. Phys. Lett. 38 (6) (2021) 066801.
[32] C. Cui, F. Xue, W.J. Hu, L.J. Li, Two-dimensional materials with piezoelectric and ferroelectric functionalities, NPJ 2D Mater. Appl. 2 (1) (2018) 18.
[33] Z. Guan, H. Hu, X. Shen, et al., Recent progress in two-dimensional ferroelectric materials, Adv. Electron. Mater. 6 (1) (2020) 1900818.
[34] L. Qi, S. Ruan, Y.J. Zeng, Review on recent developments in 2D ferroelectrics: theories and applications, Adv. Mater. 33 (13) (2021) 2005098.
[35] M. Wu, Two-dimensional van der Waals ferroelectrics: scientific and technological opportunities, ACS Nano 15 (6) (2021) 9229–9237.
[36] F. Xue, J.H. He, X. Zhang, Emerging van der Waals ferroelectrics: unique properties and novel devices, Appl. Phys. Rev. 8 (2) (2021) 021316.
[37] X. Jin, L. Tao, Y.Y. Zhang, et al., Research progress of novel properties in several van der Waals ferroelectric materials, Acta. Phys. Sin. 71 (12) (2022) 127305 -127301.
[38] M. Wu, J.D. Burton, E.Y. Tsymbal, et al., Hydroxyl-decorated graphene systems as candidates for organic metal-free ferroelectrics, multiferroics, and high-performance proton battery cathode materials, Phys. Rev. B 87 (8) (2013) 081406.
[39] M. Wu, X.C. Zeng, Bismuth oxychalcogenides: a new class of ferroelectric/ferroelastic materials with Ultra High mobility, Nano Lett. 17 (10) (2017) 6309–6314.
[40] W. Luo, K. Xu, H. Xiang, Two-dimensional hyperferroelectric metals: a different route to ferromagnetic-ferroelectric multiferroics, Phys. Rev. B 96 (23) (2017) 235415.
[41] Y. Zhao, L. Lin, Q. Zhou, et al., Surface vacancy-induced switchable electric polarization and enhanced ferromagnetism in monolayer metal trihalides, Nano Lett. 18 (5) (2018) 2943–2949.
[42] M. Xu, C. Huang, Y. Li, et al., Electrical control of magnetic phase transition in a type-I multiferroic double-metal trihalide monolayer, Phys. Rev. Lett. 124 (6) (2020) 067602.
[43] C. Xu, P. Chen, H. Tan, et al., Electric-field switching of magnetic topological charge in type-I multiferroics, Phys. Rev. Lett. 125 (3) (2020) 037203.
[44] J.J. Zhang, L. Lin, Y. Zhang, et al., Type-II multiferroic $Hf_2VC_2F_2$ MXene monolayer with high transition temperature, J. Am. Chem. Soc. 140 (30) (2018) 9768–9773.
[45] S. Zhou, L. You, H. Zhou, et al., Van der Waals layered ferroelectric $CuInP_2S_6$: physical properties and device applications, Front. Phys. 16 (1) (2020) 13301.
[46] B. Xu, H. Xiang, Y. Xia, et al., Monolayer $AgBiP_2Se_6$: an atomically thin ferroelectric semiconductor with out-plane polarization, Nanoscale 9 (24) (2017) 8427–8434.
[47] X.Y. Ma, H.Y. Lyu, K.R. Hao, et al., Large family of two-dimensional ferroelectric metals discovered via machine learning, Sci. Bull. 66 (3) (2021) 233–242.
[48] J. Qi, H. Wang, X. Chen, X. Qian, Two-dimensional multiferroic semiconductors with coexisting ferroelectricity and ferromagnetism, Appl. Phys. Lett. 113 (4) (2018) 043102.
[49] Y. Lai, Z. Song, Y. Wan, et al., Two-dimensional ferromagnetism and driven ferroelectricity in van der Waals $CuCrP_2S_6$, Nanoscale 11 (12) (2019) 5163–5170.
[50] S. Barraza-Lopez, B.M. Fregoso, J.W. Villanova, et al., Colloquium: physical properties of group-IV monochalcogenide monolayers, Rev. Mod. Phys. 93 (1) (2021) 011001.
[51] Y.T. Huang, N.K. Chen, Z.Z. Li, et al., Two-dimensional In_2Se_3: a rising advanced material for ferroelectric data storage, InfoMat 4 (8) (2022) e12341.
[52] W. Ding, J. Zhu, Z. Wang, et al., Prediction of intrinsic two-dimensional ferroelectrics in In_2Se_3 and other III_2-VI_3 van der Waals materials, Nat. Commun. 8 (1) (2017) 14956.
[53] C. Cui, W.J. Hu, X. Yan, et al., Intercorrelated in-plane and out-of-plane ferroelectricity in ultrathin two-dimensional layered semiconductor In_2Se_3, Nano Lett. 18 (2) (2018) 1253–1258.
[54] J. Xiao, H. Zhu, Y. Wang, et al., Intrinsic two-dimensional ferroelectricity with dipole locking, Phys. Rev. Lett. 120 (22) (2018) 227601.
[55] S.M. Poh, S.J.R. Tan, H. Wang, et al., Molecular-beam epitaxy of two-dimensional In_2Se_3 and its giant electroresistance switching in ferroresistive memory junction, Nano Lett. 18 (10) (2018) 6340–6346.
[56] X. Jin, Y.Y. Zhang, S.T. Pantelides, S. Du, Integration of graphene and two-dimensional ferroelectrics: properties and related functional devices, Nanoscale Horiz 5 (9) (2020) 1303–1308.
[57] C. Xu, Y. Chen, X. Cai, et al., Two-dimensional antiferroelectricity in nanostripe-ordered In_2Se_3, Phys. Rev. Lett. 125 (4) (2020) 047601.
[58] Z. Zhang, J. Nie, Z. Zhang, et al., Atomic visualization and switching of ferroelectric order in β-In_2Se_3 films at the single layer limit, Adv. Mater. 34 (3) (2022) 2106951.
[59] S. Yuan, X. Luo, H.L. Chan, et al., Room-temperature ferroelectricity in $MoTe_2$ down to the atomic monolayer limit, Nat. Commun. 10 (1) (2019) 1775.
[60] S.N. Shirodkar, U.V. Waghmare, Emergence of ferroelectricity at a metal-semiconductor transition in a 1T monolayer of MoS_2, Phys. Rev. Lett. 112 (15) (2014) 157601.
[61] K. Yasuda, X. Wang, K. Watanabe, et al., Stacking-engineered ferroelectricity in bilayer boron nitride, Science 372 (6549) (2021) 1458–1462.
[62] M. Vizner Stern, Y. Waschitz, W. Cao, et al., Interfacial ferroelectricity by van der Waals sliding, Science 372 (6549) (2021) 1462–1466.
[63] L. Li, M. Wu, Binary compound bilayer and multilayer with vertical polarizations: two-dimensional ferroelectrics, multiferroics, and nanogenerators, ACS Nano 11 (6) (2017) 6382–6388.
[64] Q. Yang, M. Wu, J. Li, Origin of two-dimensional vertical ferroelectricity in WTe_2 bilayer and multilayer, J. Phys. Chem. Lett. 9 (24) (2018) 7160–7164.
[65] Z. Fei, W. Zhao, T.A. Palomaki, et al., Ferroelectric switching of a two-dimensional metal, Nature 560 (7718) (2018) 336–339.
[66] Y. Liang, S. Shen, B. Huang, et al., Intercorrelated ferroelectrics in 2D van der Waals materials, Mater. Horiz. 8 (6) (2021) 1683–1689.
[67] A. Chandrasekaran, A. Mishra, A.K. Singh, Ferroelectricity, antiferroelectricity, and ultrathin 2D electron/hole gas in multifunctional monolayer MXene, Nano Lett. 17 (5) (2017) 3290–3296.
[68] L. Zhang, C. Tang, C. Zhang, A. Du, First-principles screening of novel ferroelectric MXene phases with a large piezoelectric response and unusual auxeticity, Nanoscale 12 (41) (2020) 21291–21298.
[69] X. Jin, L. Tao, Y.Y. Zhang, et al., Intrinsically scale-free ferroelectricity in two-dimensional $M_2X_2Y_6$, Nano Res. 15 (4) (2022) 3704–3710.
[70] K.R. Hao, X.Y. Ma, Z. Zhang, et al., Ferroelectric and room-temperature ferromagnetic semiconductors in the 2D $M_IM_{II}Ge_2X_6$ family: first-principles and machine learning investigations, J. Phys. Chem. Lett. 12 (41) (2021) 10040–10051.
[71] K.R. Hao, X.Y. Ma, H.Y. Lyu, et al., The atlas of ferroicity in two-dimensional $MGeX_3$ family: room-temperature ferromagnetic half metals and unexpected ferroelectricity and ferroelasticity, Nano Res. (2021).
[72] C. Zheng, L. Yu, L. Zhu, et al., Room temperature in-plane ferroelectricity in van der Waals In_2Se_3, Sci. Adv. 4 (7) (2018) eaar7720.
[73] R.D. King-Smith, D. Vanderbilt, Theory of polarization of crystalline solids, Phys. Rev. B 47 (3) (1993) 1651–1654.
[74] D. Vanderbilt, R.D. King-Smith, Electric polarization as a bulk quantity and its relation to surface charge, Phys. Rev. B 48 (7) (1993) 4442–4455.
[75] R. Resta, Theory of the electric polarization in crystals, Ferroelectrics 136 (1) (1992) 51–55.
[76] R. Resta, Macroscopic polarization in crystalline dielectrics: the geometric phase approach, Rev. Mod. Phys. 66 (3) (1994) 899–915.
[77] S.C. de la Barrera, Q. Cao, Y. Gao, et al., Direct measurement of ferroelectric polarization in a tunable semimetal, Nat. Commun. 12 (1) (2021) 5298.
[78] P. Sharma, F.X. Xiang, D.F. Shao, et al., A room-temperature ferroelectric semimetal, Sci. Adv. 5 (7) (2019) eaax5080.

[79] D. Puggioni, J.M. Rondinelli, Designing a robustly metallic noncenstrosymmetric ruthenate oxide with large thermopower anisotropy, Nat. Commun. 5 (1) (2014) 3432.
[80] A. Filippetti, V. Fiorentini, F. Ricci, et al., Prediction of a native ferroelectric metal, Nat. Commun. 7 (1) (2016) 11211.
[81] W.X. Zhou, A. Ariando, Review on ferroelectric/polar metals, Jpn. J. Appl. Phys. 59 (SI) (2020) SI0802.
[82] S. Lizzit, R. Larciprete, P. Lacovig, et al., Transfer-free electrical insulation of epitaxial graphene from its metal substrate, Nano Lett. 12 (9) (2012) 4503–4507.
[83] Z.Y. Al Balushi, K. Wang, R.K. Ghosh, et al., Two-dimensional gallium nitride realized via graphene encapsulation, Nat. Mater. 15 (2016) 1166.
[84] G. Li, L. Zhang, W. Xu, et al., Stable silicene in graphene/silicene van der Waals heterostructures, Adv. Mater. 30 (49) (2018) 1804650.
[85] J. Mao, L. Huang, Y. Pan, et al., Silicon layer intercalation of centimeter-scale, epitaxially grown monolayer graphene on Ru(0001), Appl. Phys. Lett. 100 (9) (2012) 093101.
[86] L. Omiciuolo, E.R. Hernández, E. Miniussi, et al., Bottom-up approach for the low–cost synthesis of graphene-alumina nanosheet interfaces using bimetallic alloys, Nat. Commun. 5 (1) (2014) 5062.
[87] H. Guo, X. Wang, L. Huang, et al., Insulating SiO_2 under centimeter-scale, single-crystal graphene enables electronic-device fabrication, Nano Lett. 20 (12) (2020) 8584–8591.
[88] C. Baeumer, D. Saldana-Greco, J.M.P. Martirez, et al., Ferroelectrically driven spatial carrier density modulation in graphene, Nat. Commun. 6 (1) (2015) 6136.
[89] B. Huang, G. Clark, E. Navarro-Moratalla, et al., Layer-dependent ferromagnetism in a van der Waals crystal down to the monolayer limit, Nature 546 (7657) (2017) 270–273.
[90] C. Gong, L. Li, Z. Li, et al., Discovery of intrinsic ferromagnetism in two-dimensional van der Waals crystals, Nature 546 (7657) (2017) 265–269.
[91] Y. Deng, Y. Yu, Y. Song, et al., Gate-tunable room-temperature ferromagnetism in two-dimensional Fe_3GeTe_2, Nature 563 (7729) (2018) 94–99.
[92] Z. Yu, W. Xia, K. Xu, et al., Pressure-induced structural phase transition and a special amorphization phase of two-dimensional ferromagnetic semiconductor $Cr_2Ge_2Te_6$, J. Phys. Chem. C 123 (22) (2019) 13885–13891.
[93] W. Ge, K. Xu, W. Xia, et al., Raman spectroscopy and lattice dynamical stability study of 2D ferromagnetic semiconductor $Cr_2Ge_2Te_6$ under high pressure, J. Alloys Compd. 819 (2020) 153368.
[94] Y. Shuang, S. Hatayama, H. Tanimura, et al., Nitrogen doping-induced local structure change in a $Cr_2Ge_2Te_6$ inverse resistance phase-change material, Mater. Adv. 1 (7) (2020) 2426–2432.
[95] X. Jin, First-Principles Studies of Several Two-Dimensional Ferroelectric Materials and Related Heterostructures, University of Chinese Academy of Sciences, 2022.
[96] H.J. Lee, M. Lee, K. Lee, et al., Scale-free ferroelectricity induced by flat phonon bands in HfO_2, Science 369 (6509) (2020) 1343.
[97] G. Constantinescu, A. Kuc, T. Heine, Stacking in bulk and bilayer hexagonal boron nitride, Phys. Rev. Lett. 111 (3) (2013) 036104.
[98] S. Zhou, J. Han, S. Dai, et al., van der Waals bilayer energetics: generalized stacking-fault energy of graphene, boron nitride, and graphene/boron nitride bilayers, Phys. Rev. B 92 (15) (2015) 155438.
[99] S.M. Gilbert, T. Pham, M. Dogan, et al., Alternative stacking sequences in hexagonal boron nitride, 2D Mater. 6 (2) (2019) 021006.
[100] C. Gong, E.M. Kim, Y. Wang, et al., Multiferroicity in atomic van der Waals heterostructures, Nat. Commun. 10 (1) (2019) 2657.
[101] Y. Lu, R. Fei, X. Lu, et al., Artificial multiferroics and enhanced magnetoelectric effect in van der Waals heterostructures, ACS Appl. Mater. Interfaces 12 (5) (2020) 6243–6249.
[102] W. Sun, W. Wang, D. Chen, et al., Valence mediated tunable magnetism and electronic properties by ferroelectric polarization switching in 2D FeI_2/In_2Se_3 van der Waals heterostructures, Nanoscale 11 (20) (2019) 9931–9936.
[103] C.K. Li, X.P. Yao, G. Chen, Writing and deleting skyrmions with electric fields in a multiferroic heterostructure, Phys. Rev. Res. 3 (1) (2021) L012026.
[104] W. Sun, W. Wang, H. Li, et al., Controlling bimerons as skyrmion analogues by ferroelectric polarization in 2D van der Waals multiferroic heterostructures, Nat. Commun. 11 (1) (2020) 5930.
[105] W. Sun, W. Wang, J. Zang, et al., Manipulation of magnetic skyrmion in a 2D van der Waals heterostructure via both electric and magnetic fields, Adv. Funct. Mater. 31 (47) (2021) 2104452.
[106] X. Jin, A. O'Hara, Y.Y. Zhang, et al., Designing strong and tunable magnetoelectric coupling in 2D trilayer heterostructures, 2D Mater. 10 (1) (2023) 015007.
[107] X.W. Shen, W.Y. Tong, S.J. Gong, C.G. Duan, Electrically tunable polarizer based on 2D orthorhombic ferrovalley materials, 2D Mater. 5 (1) (2017) 011001.
[108] S. Picozzi, Ferroelectric Rashba semiconductors as a novel class of multifunctional materials, Front. Phys. 2 (2014) 10.
[109] J. Chen, K. Wu, W. Hu, J. Yang, Spin–orbit coupling in 2D semiconductors: a theoretical perspective, J. Phys. Chem. Lett. 12 (51) (2021) 12256–12268.
[110] J.J. Zhang, D. Zhu, B.I. Yakobson, Heterobilayer with ferroelectric switching of topological state, Nano Lett. 21 (1) (2021) 785–790.
[111] Y. Liang, N. Mao, Y. Dai, et al., Intertwined ferroelectricity and topological state in two-dimensional multilayer, NPJ Comput. Mater. 7 (1) (2021) 172.

Xin Jin is now a postdoctoral researcher in University of Chinese Academy of Sciences. He received his Ph.D. degree in Condensed Matter Physics in 2022 from University of Chinese Academy of Sciences. His-research interest focus on first-principles study of nanostructures, low dimensional functional materials.

Shixuan Du is currently a professor and group leader at the Institute of Physics, Chinese Academy of Sciences. Her research interests focus on the of multidiscipline modeling of nanostructures, low dimensional materials, surfaces and interfaces.